31st Annual International Conference of the IEEE EMBS
Minneapolis, Minnesota, USA, September 2-6, 2009

Characterization of the Stress-Strain Relationship of the Abdominal Aortic Wall *In Vivo*

Asawinee Danpinid[1], Jianwen Luo[2], *Member, IEEE,* Jonathan Vappou[2], Pradit Terdtoon[1] and Elisa E. Konofagou[2] , *Member, IEEE*
[1]Department of Mechanical Engineering, Chiang Mai University, Chiang Mai, THAILAND
[2]Department of Biomedical Engineering, Columbia University, New York, NY, USA
ek2191@columbia.edu

Abstract*—We hereby propose a new method to determine the regionally passive, elastic, stress-strain relationship of the normal murine abdominal aorta *in vivo*. The circumferential stress-strain relationship was assessed through Laplace's law, a small deformation framework and a relationship between luminal pressure and diameter variation. The regional diameter variation of the murine abdominal aortas was obtained using a cross-correlation technique on radio-frequency (RF) signals at the extremely high frame rate of 8 kHz. The luminal pressure variation was measured by an ultra-miniature pressure catheter over one cardiac cycle. The change of slope of the stress-strain curve was noticed, which was the contribution of elastin and engaged collagen fibers. The stress-strain relationships before and after this transition was assumed to be linear. Three Young's moduli of the aortic wall were characterized in six mice *in vivo*: (1) elastin, (2) elastin-collagen and (3) engaged collagen fibers, which were equal to 91.6±26.5, 229.0±80.4 and 137.5±65.6 kPa, respectively. The proposed methodology thus allowed for noninvasive mapping of the mechanical properties of its constituents *in vivo.

Keywords –aorta; collagen; elastin; stress-strain relationship; vascular diseases; ultrasound

I. Introduction

Arterial stiffness has been used as a predictive indicator of cardiovascular disease [1]. The stiffness can be determined from the underlying stress-strain relationship. For this reason, numerous constitutive models of the aorta have been previously established and developed for fundamental biomechanical understanding, diagnostic or clinical treatment [2]. They were established based on *in vitro* experiments, where certain characteristics can be completely different from their physiologic conditions. Therefore, it can be extremely challenging to characterize the equivalent vascular stress-strain relationship *in vivo,* which requires investigating physiologic condition.

Several definitions of arterial stiffness have been proposed in order to identify vascular abnormalities *in vivo*. They were derived from radial pulsation at the end-systolic and end-diastolic phases [3]. For instance, the aortic compliance has been defined as the ratio of the vessel diameter to the luminal pressure. The pressure-strain elastic modulus (E_p) equal to the inverse of the compliance multiplied by the end-diastolic diameter. The stiffness index (β) is equal to the ratio of logarithmic of luminal pressure to the vessel diameter multiplied by the end-diastolic diameter. Although they all provide qualitative information on the stiffness in general, these moduli represent only one specific value, i.e., not the stress-strain relationship. The stress-strain relationship provides further information including the effects of the different wall constituents [4, 5]. It can provide important constitutional information on the mechanical behavior through the aortic stress-strain relationship.

To obtain the *in vivo* aortic wall stress-strain relationship, experimental data are required. There are several techniques to measure luminal pressure and wall geometry change *in vivo* [6]. The luminal pressure is obtained by an invasive measurement with a pressure catheter inserted into the aortic lumen [3, 6, 7]. Generally, the wall geometry and motion can be detected non-invasively by MRI (Magnetic Resonance Imaging) and ultrasound imaging [8]. Although MRI provides detailed images, it is typically associated with low temporal resolution. Ultrasound can provide high spatial and temporal resolution, which is widely applied in medical diagnosis. Luo *et al.* (2009) proposed the Pulse Wave Imaging (PWI) technique to visualize the pulse wave non-invasively by using ultrasound radio-frequency (RF) signals. This non-invasive *in vivo* technique has been proven very effective for displacement measurement.

In this study, our goal is to develop a new method to fully characterize the passive stress-strain relationship *in vivo* with normal physiologic conditions by using the pressure measurement and the ultrasound-based wall motion estimation. The luminal pressure variation was measured using a pressure catheter. The radial wall motion was captured using a 1D cross-correlation technique. The murine abdominal aorta was selected because of its simple geometry and association with critical vascular diseases such as aneurysm and atherosclerosis. The abdominal aortic wall was assumed to be cylindrically isotropic, homogeneous and incompressible. The perivascular tissue effect was ignored.

II. Methods

A. Model description

In this study, the abdominal aortic configuration was assumed to be a perfectly cylindrical tube, radially inflated by the luminal pressure. The extravascular pressure was

This study was supported in part by the National Institutes of Health (R01EB006042), the Fulbright Association and the Thailand Research Fund.

assumed to be zero. Laplace's law was used for the mean circumferential stress calculation, i.e.,

$$\sigma_\theta(t) = \frac{P_i(t) d_i(t)}{d_o(t) - d_i(t)} \quad (1)$$

where σ_θ is the mean circumferential stress and P_i, d_i, d_o are the luminal pressure, and the inner and outer diameter of the aortic wall, respectively. The stretch ratio, λ_θ, is the circumferential strain [6, 9], i.e.,

$$\lambda_\theta(t) = \frac{d_{mean}(t)}{D_{mean}} \quad (2)$$

where $d_{mean}(t) = (d_i(t)+d_o(t))/2$ is the mean aortic diameter and D_{mean} is the *in vivo* reference configuration defined as the minimum vessel diameter over a cardiac cycle.

In fact, the aorta consists of a meshed matrix of elastin and collagen fibers, vascular smooth muscle cells, and connective tissue. The passive elastic behavior of the aortic wall is mainly influenced by the elastin and collagen fibers [4, 10]. The transition from the act of elastin to collagen fibers is called "breaking point" [4]. We hypothesized that at low physiologic pressures, the elastin layers would dilate due to the luminal pressure until they reached the breaking point ($\lambda_{\theta,0}$). E_1 was defined as the Young's modulus of the elastin [6, 9]. At the breaking point, we assumed that a number of activated collagen fibers became engaged while the elastin layers continued to expand. The subsequent activated collagen fibers had lower stiffness compared to the formerly activated collagen fibers. Therefore, the stress-strain relationship after the breaking point was approximated as the Young's modulus, i.e., E_2. This was assumed to be a good approximation, as it was applied on blood vessels in several previously reported studies [4, 5]. The phenomenological model was assumed to be a parallel spring model (Fig. 1B) [4, 10] following the lamellae structure arrangement (Fig. 1A). The circumferential stress was assumed as follows:

$$\sigma_\theta(t) = \begin{cases} E_1 \lambda_\theta(t) & : 1 \le \lambda_\theta \le \lambda_{\theta,0} \quad (3.1) \\ E_2 \lambda_\theta(t) = E_1 \lambda_\theta(t) + E_3 \left(\lambda_\theta(t) - \lambda_{\theta,0}\right) & : \lambda_{\theta,0} \le \lambda_\theta \quad (3.2) \end{cases}$$

The Young's modulus of engaged collagen fibers was considered equal to E_3. At each longitudinal location, the first two Young's moduli, E_1 and E_2 were assessed. E_3 was estimated as follows

$$E_3 = E_2 - E_1 \quad (4)$$

Therefore, the Young's moduli were estimated using our method: 1) elastin (E_1), 2) elastin-collagen (E_2) and 3) engaged collagen fibers (E_3). To compute the Young's moduli, luminal pressure and diameter variations of the aortic wall were measured.

B. Experimental procedure

A murine abdominal aorta was canulated using an ultra-miniature pressure catheter (SciSense, London, ON, Canada) through the mouse's carotid artery and introduced into the abdominal aortic region. The ECG was acquired using the electrode leads available on the heating mouse platform (THM100, Indus, Instruments, Houston, TX). Both luminal pressure and ECG signals were acquired by using a two-channel 14-bit waveform digitizer (CompuScope 14200, Gage Applied Technologies Inc., Lachine, QC, Canada) at sampling frequency of 10 kHz. Six mice were used for wall deformation measurement in this study. A 30-MHz ultrasound probe (RMV-707B, VisualSonics Inc., Toronto, ON, Canada) was placed on the murine abdomen. A longitudinal (long-axis) view of the abdominal aorta was used so as to align the radial direction of the aorta with the axial direction of the ultrasound beams. Following data acquisition, the acquired RF signals were gated between two consecutive R-waves to reconstruct the image sequence for a complete cardiac cycle at the extremely high frame rate of 8 kHz. Along an abdominal aortic length of 12 mm, the incremental (i.e., between consecutive RF frames), axial (i.e., along the direction of ultrasound propagation) displacements, parallel to the radial direction of the abdominal aorta, were estimated off-line using a one-dimensional (1-D) normalized cross-correlation technique on the acquired RF signals [11].

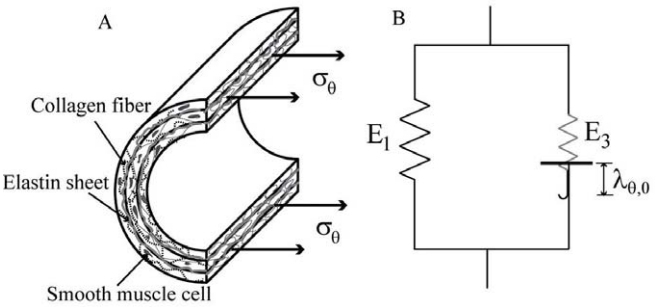

Fig. 1. (A) Lamellae arrangement representation of elastin, collagen fibers and smooth muscle cells in aorta and (B) the phenomenological model used in this study.

C. Parameter calculations

A single luminal pressure profile in a specific aortic region was assumed to represent the pressure over the entire scanned abdominal region corresponding to the diameter variation in every longitudinal location of the abdominal aorta. The inner and outer aortic diameters and abdominal aortic wall regions were clearly obtained though manual tracing on the B-mode image by a trained observer (Fig. 2A). The radial incremental displacements of the inner and outer walls were then calculated (Fig. 2B). These were accumulated to obtain the wall diameter variation over one cardiac cycle. The luminal pressure and aortic wall diameter variations were matched using the corresponding ECG. Since the aortic wall behavior was assumed to be purely elastic, the phase shift between the pressure and diameter variations, resulting from viscoelastic behavior, was ignored. Hence, the maximum and minimum peaks of the luminal pressure and diameter variations were aligned. The aortic dilation, i.e., from the minimum to maximum diameter peak, was measured in order to interpret the aortic passive

behavior. The circumferential stress, strain and the three Young's moduli were computed based on the model at every longitudinal location as shown in Eqs. (3) and (4).

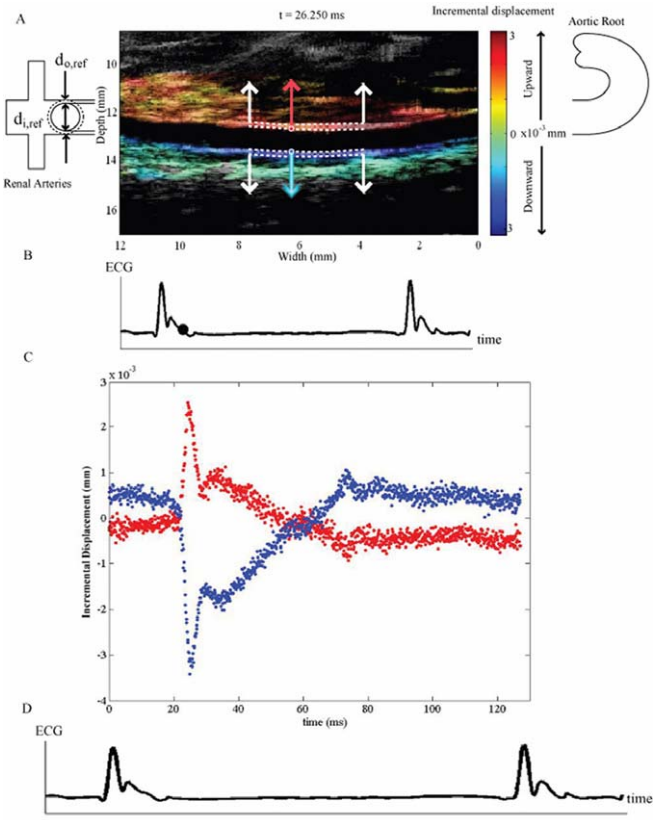

Fig. 2. (A) The B-mode image of the murine abdominal aorta. (B) The black dot on the ECG denotes the phase at which the image in (A) was acquired. (C) The incremental displacements at an arbitrary location over a single cardiac cycle. Red and blue dots indicate the locations of the ventral and dorsal aortic walls, respectively. (D)The incremental displacements in (C) were taken over a cardiac cycle.

III. Results and Discussion

Fig. 3 shows the calculated stress-strain relationship of the abdominal aortic wall in a specific location on the aortic wall of a mouse i*n vivo*. At low strain levels, the stress is gradually increased until it reaches a breaking point, $\lambda_{\theta,0}$, beyond which the slope changes. This phenomenon was observed at every longitudinal location of the selected region (Fig. 4). The represented Young's moduli in each mouse are shown in Table I, as a mean value and standard deviation over the selected locations.

The average E_1 value (Table 1) was 1.5-2 times higher than the mechanical testing values in the rat aorta *in vitro* [12], i.e., about 40-60 kPa. This is probably because of the difference between *in vitro* and *in vivo* conditions. Also the elastic modulus in [12] corresponded to the two-constituents model, which was assumed to be Neo-Hookean material. This is equivalent to Hooke's law in the large deformation framework [13].

E_2, the elastin-collagen modulus (Table I), was also compared to previously reported stiffness values measured.

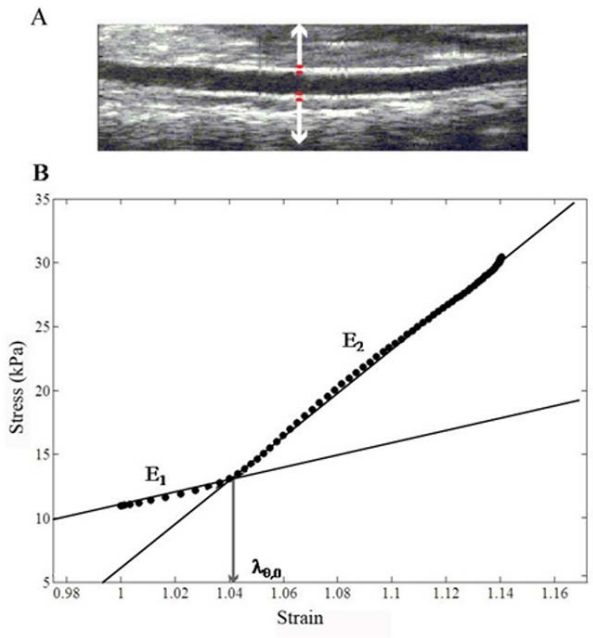

Fig. 3. (A) Selected aortic wall region (B) Circumferential stress versus aortic wall strain with E_1, E_2 and the breaking point, ($\lambda_{\theta,0}$).

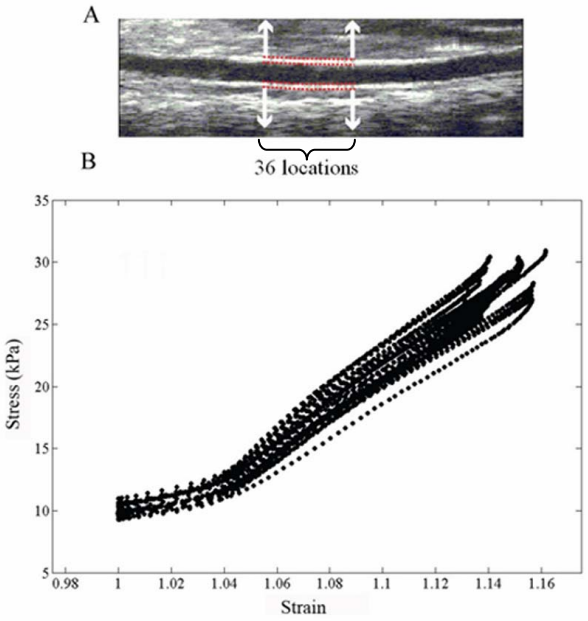

Fig. 4. (A) Longitudinal measurements of the aortic wall (B) The circumferential stress versus strain from the aorta dilation in 36 locations as shown in (A).

Other studies on rats and mice *in vivo* have reported 3 to 6 times higher stiffness that in the normal case [14-16]. This may be because only the medial layer was taken into account in their study. The thickness was also measured *in vitro*, which can be ten times lower since the vessel is no longer pressurized. The wall thickness is an important factor in the calculation of the elastic modulus that our method can obtain accurately B-mode ultrasound imaging (Fig. 2A).

Regarding the E_3 value, it corresponded to the engagement of collagen fibers and other wall constituents *in vivo*. This could not be compared to the value proposed by

[12] since only the modulus of pure collagen was 200 MPa (referred to c_{coll} in [12]). However, E_3 was found to be higher than E_1 (Table I). This is in line with previous reports where the elastic modulus of collagen was shown to be significantly higher than that of the elastin [3, 7].

TABLE I
Young's moduli of E_1, E_2 and E_3 in the abdominal aortic wall

Mouse	E_1 (kPa)	E_2 (kPa)	E_3 (kPa)
1	124.9±10.2	225.7±18.9	100.8±8.8
2	57.3±3.7	144.1±4.2	86.9±7.6
3	85.7±15.1	170.7±62.6	85.0±52.5
4	94.0±7.3	322.3±21.6	228.3±14.4
5	69.6±12.8	179.7±28.9	110.1±16.2
6	117.9±12.1	331.8±31.9	213.9±20.9
Average	91.6±26.5	229.0±80.4	137.5±65.6

The proposed method can be compared to previously reported studies [4, 5, 7]. For example, Intravascular Ultrasound (IVUS) palpography has been employed to monitor the wall deformation. It is an invasive method, which cannot always be used for diagnostic purposes. Our non-invasive imaging technique also detected the aortic wall deformation at every longitudinal location [11].

However, there are limitations in the proposed methodology. First, we assumed the extravascular pressure to be zero. The passive behavior of the aortic wall may be affected by connective tissues, ignored in this study [10]. Second, the viscosity of the wall was also ignored. Therefore, the Young's modulus value approximated only the elastic property of the aorta. Third, the luminal pressure was measured in different mice from those used in this study. The difference in heart rate, respiratory rate and other physiologic factors may influence the stress-strain relationship. The pressure was assumed to be uniform across the entire vessel. This assumption may affect the magnitude of the calculated circumferential stress.

However, catheterization of the mouse aorta for luminal pressure measurements can be extremely challenging. It may be impossible to obtain the exact luminal pressure *in vivo* because the presence of the catheter in the lumen will affect the flow and pressure experienced by the wall. We may avoid these effects by using non-invasive carotid or brachial pressure measurements. Even though these pressures are different from those in the aorta, at least the blood pressure waveform can be known. It could be corrected using Doppler flow measurements in the future studies.

Despite the aforementioned limitations, the proposed method provides the basic mechanical properties of the abdominal aortic wall by taking into account the influence of its constituents *in vivo*. It does not only provide the regional aortic Young's moduli of its different constituents but also identify the breaking point from elastin to collagen. This may then provide a unique fundamental understanding on the elastic behavior of the vessel *in vivo*. This method could be used to monitor the change of the vascular wall function with disease or aging. For example, it is expected that the modulus of elastin lamellae will be affected by aging, aneurysm or atherosclerosis.

IV. CONCLUSIONS

The linear stress-strain relationship provides a good approximation on the physiologic function of the aorta. The regional material parameters provided a reliable index for diagnostic purposes and the methodology could be applied as a useful tool for clinical diagnosis. Therefore, our method provides a way to determine the regional stress-strain relationship non-invasively for detecting and monitoring vascular disease *in vivo*.

ACKNOWLEDGMENT

We are grateful to Kana Fujikura, M.D. PhD., from Columbia University and Jawad Latif, M.D., from St. Luke's-Roosevelt Hospital Center, for conducting the experiments. We also thank Phrut Sakulchangsatjatai, Ph.D., Chiang Mai University, for all helpful discussions.

REFERENCES

[1] A. J. Hall, E. F. G. Busse, D. J. McCarville, and J. J. Burgess, *Annals of Vascular Surgery,* vol. 14, pp. 152-157, 2000.

[2] R. P. Vito and S. A. Dixon, *Annual Review of Biomedical Engineering,* vol. 5, pp. 413-439, 2003.

[3] W. W. Nichols, M. F. O'Rourke, and D. A. McDonald, London: E. Arnold, 1990.

[4] R. L. Armentano, J. Levenson, J. G. Barra, E. I. Fischer, G. J. Breitbart, R. H. Pichel, and A. Simon, *Am J Physiol Heart Circ Physiol,* vol. 260, pp. H1870-1877, 1991.

[5] J. G. Barra, R. L. Armentano, J. Levenson, E. I. Fischer, R. H. Pichel, and A. Simon, *Circ Res,* vol. 73, pp. 1040-1050, 1993.

[6] J. D. Humphrey, *Cardiovascular solid mechanics : cells, tissues, and organs*. New York: Springer, 2002.

[7] R. L. Armentano, J. G. Barra, J. Levenson, A. Simon, and R. H. Pichel, *Circ Res,* vol. 76, pp. 468-478, 1995.

[8] I. S. Mackenzie, I. B. Wilkinson, and J. R. Cockcroft, *QJM,* vol. 95, pp. 67-74, 2002.

[9] Y.-c. Fung, New York, NY ;Berlin [u.a.]: Springer, 1993.

[10] R. H. Cox, *Am J Physiol Heart Circ Physiol,* vol. 234, pp. H533-541, 1978.

[11] J. Luo, K. Fujikura, L. S. Tyrie, M. D. Tilson, and E. E. Konofagou, *Medical Imaging, IEEE Transactions on,* vol. 28, pp. 477-486, 2009.

[12] M. A. M. A. Zulliger, P. Fridez, K. Hayashi, and N. Stergiopulos, *Journal of Biomechanics,* vol. 37, pp. 989-1000, 2004.

[13] H.-C. Wu, Boca Raton: Chapman & Hall/CRC, 2005.

[14] V. Marque, P. Kieffer, B. Gayraud, I. Lartaud-Idjouadiene, F. Ramirez, and J. Atkinson, *Arterioscler Thromb Vasc Biol,* vol. 21, pp. 1184-1189, 2001.

[15] P. Lacolley, C. Labat, A. Pujol, C. Delcayre, A. Benetos, and M. Safar, *Circulation,* vol. 106, pp. 2848-2853, 2002.

[16] Y. Bezie, J.-M. D. Lamaziere, S. Laurent, P. Challande, R. S. Cunha, J. Bonnet, and P. Lacolley, *Arterioscler Thromb Vasc Biol,* vol. 18, pp. 1027-1034, 1998.